Mononuclear Platinum(II) and Palladium(II) Dithiolate Complexes as Chelate Metalloligands for Preparation of Heterobimetallic d^8-d^8 Complexes

Jorge Forniés-Cámer,[†] Anna M. Masdeu-Bultó,[†] Carmen Claver,*[,†] and Christine J. Cardin[‡]

Departament de Química, Universitat Rovira i Virgili, Pl. Imperial Tarraco, 1, 43005 Tarragona, Spain, and Department of Chemistry, The University of Reading, Whiteknights, P.O. Box 224, Reading RG6 6AD, U.K.

Received May 9, 1997

Palladium−rhodium and platinum−rhodium heterobimetallic bridged dithiolate complexes of general formula $[(P-P)M(\mu\text{-}S-S)Rh(COD)]ClO_4$ (COD = 1,5-cyclooctadiene. For M = Pt: P−P = $(PPh_3)_2$ and S−S = EDT^{2-} (1,2-ethanedithiolate) (**1**), PDT^{2-} (1,3-propanedithiolate) (**2**), and BDT^{2-} (1,4-buthanedithiolate) (**3**); P−P = dppb (1,4-bis(diphenylphosphino)butane) and S−S = EDT^{2-} (**4**), PDT^{2-} (**5**), and BDT^{2-} (**6**); P−P = dppp (1,3-bis-(diphenylphosphino)propane) and S−S = EDT^{2-} (**7**), PDT^{2-} (**8**), and BDT^{2-} (**9**). For M = Pd: P−P = dppb and S−S = EDT^{2-} (**10**), PDT^{2-} (**11**), and BDT^{2-} (**12**); P−P = dppp and S−S = EDT^{2-} (**13**), PDT^{2-} (**14**), and BDT^{2-} (**15**)) have been prepared. The crystal structures for complexes **1**−**3**, **6**, **9**, and **12** have been determined, and hinged structures were found with angles between local coordination planes MS_2Rh ranging from 111.27° for complex **1** to 151.34° for complex **3**. Metal−metal distances show nonbonding interactions between metals. X-ray data for **1**: triclinic, $P\bar{1}$, $a = 11.311(6)$ Å, $b = 12.991(6)$ Å, $c = 16.140(6)$ Å, $\alpha = 84.86(6)°$, $\beta = 75.73(6)°$, $\gamma = 86.43(6)°$, $Z = 2$, $R = 0.0427$ ($R_w = 0.1151$). X-ray data for **2**: triclinic, $P\bar{1}$, $a = 11.084(5)$ Å, $b = 13.094(6)$ Å, $c = 16.338(6)$ Å, $\alpha = 86.06(6)°$, $\beta = 75.67(6)°$, $\gamma = 88.55(6)°$, $Z = 2$, $R = 0.0470$ ($R_w = 0.1264$). X-ray data for **3**: orthorhombic, *Pbca*, $a = 14.439(6)$ Å, $b = 19.807(6)$ Å, $c = 38.156(6)$ Å, $Z = 8$, $R = 0.0864$ ($R_w = 0.2457$). X-ray data for **6**: monoclinic, $P2_1/c$, $a = 20.338(6)$ Å, $b = 14.227(6)$ Å, $c = 14.570(6)$ Å, $\beta = 100.94(6)°$, $Z = 4$, $R = 0.0536$ ($R_w = 0.1449$). X-ray data for **9**: monoclinic, $P2_1/c$, $a = 20.326(6)$ Å, $b = 14.109(6)$ Å, $c = 14.368(6)$ Å, $\beta = 100.90(6)°$, $Z = 4$, $R = 0.0380$ ($R_w = 0.0990$). X-ray data for **12**: monoclinic, $P2_1/c$, $a = 20.365(6)$ Å, $b = 14.186(6)$ Å, $c = 14.592(6)$ Å, $\beta = 101.04(6)°$, $Z = 4$, $R = 0.0507$ ($R_w = 0.1500$).

Introduction

Interest in homo- and hetero-bimetallic complexes has increased in the last few years due to the fact that the reactivity and properties of a metal may be strongly modified by the presence of another metallic center in close proximity. Two bonded or close nonbonded metal atoms may react in a cooperative manner with substrate molecules.[1] Furthermore, the electrochemical behavior of one metallic center may be modified by the presence of a different metal in the same molecule bonded directly or connected through a bridging ligand that may act as an electron transmitter.[2] Moreover, heterobimetallic complexes are of great interest as starting materials for the preparation of cluster compounds.[1a]

Heterobimetallic complexes have mainly been prepared by using mono- or bidentate bridging ligands which favor metal−metal interaction. Of the bidentate ligands, a major role has been played by the homodonor neutral diphosphine $Ph_2PCH_2PPh_2$ (dppm),[3] containing the donor structural unit P−C−P. This approach can be modified by using heterodonor ligands with disymmetric structural donor units such as N−C−P[3,4] (pyridine−phosphine), As−C−P[5] (arsino−phosphine), and N−C−S[6] (benzothiazole−2-thiolate), the last of which is anionic. Heterodonor ligands are especially appropriate for the synthesis of hetero-bimetallic complexes, but their disymmetric nature can yield two possible arrangements: head-to-head or head-to-tail.

Monodentate bridging ligands such as anionic thiolates (RS^-)[7] separate the metals by one atom and provide flexible structures that support a wide range of bonding and nonbonding metal−metal distances. However, the substituents, when present on the donor sulfur atom, can adopt different relative orientations, and thus complexes can have the *syn* and *anti* configurations. Therefore, the structures of dinuclear complexes, homo- or hetero-bimetallic with monothiolate bridged ligands, are rather flexible, and their structures can range from planar to bent, with

[†] Universitat Rovira i Virgili.
[‡] The University of Reading.

(1) (a) Braunstein, P.; Rose, J. In *Comprehensive Organometallic Chemistry*; Wilkinson, G., Stone, F. G. A., Abel, E. W., Eds.; Pergamon: Oxford, U.K., 1995; Vol. 10. (b) Savin, A.; Hengtai, Y.; Chaquin, P. *J. Organomet. Chem.* **1984**, *262*, 391. (c) Poilblanc, R. *Inorg. Chim. Acta* **1982**, *62*, 75.
(2) Zhou, M.; Xu, Y.; Tan, A.-M.; Leung, P.-H.; Mok, K. F.; Koh, L.-L.; Hor, T. S. A. *Inorg. Chem.* **1995**, *34*, 6425.
(3) (a) Balch, A. L. In *Homogeneous Catalysis with Metal Phosphine Complexes*; Pignolet, L. H., Ed.; Plenum Press: New York, 1983; pp 167−213. (b) Chaudret, B.; Delavaux, B.; Poilblanc, R. *Coord. Chem. Rev.* **1988**, *86*, 191.
(4) Farr, J. P.; Olmstead, M. M.; Wood, F. E.; Rutherford, N. M.; Balch, A. L. *Organometallics* **1983**, *2*, 1758 and references cited therein.
(5) (a) Balch, A. L.; Guimerans, R. R.; Linehan, J.; Wood, F. E. *Inorg. Chem.* **1985**, *24*, 2021. (b) Balch, A. L.; Guimerans, R. R.; Linehan, J.; Olmstead, M. M.; Oram, D. E. *Organometallics* **1985**, *4*, 1445.
(6) Ciriano, M. A.; Pérez-Torrente, J. J.; Lahoz, F. J.; Oro, L. A. *Inorg. Chem.* **1992**, *31*, 969, and references cited therein.
(7) (a) Jain, V. K. *Inorg. Chim. Acta.* **1987**, *133*, 261. (b) Capdevila, M.; Gonzalez-Duarte, P.; Foces-Foces, C.; Hernández Cano, F.; Martínez-Ripoll, M. *J. Chem. Soc., Dalton Trans.* **1990**, 143. (c) Amador, U.; Delgado, E.; Forniés, J.; Hernández, E.; Lalinde, E.; Moreno, M. T. *Inorg. Chem.* **1995**, *34*, 5279.

S0020-1669(97)00557-0 CCC: $15.00
Published on Web 05/06/1998

hinged angles between local coordination planes MS_2M (θ) less than 180°.[8] The distances between the metals are longer when the structure is planar, so metal−metal interactions are less favored. Even for bent structures, the estimated barrier energies of the hinge motion are low[8] and intermetallic interactions, if there are any, are frequently weak in these kinds of complexes.[9]

The use of alkyl dithiolates, $^-S(CH_2)_nS^-$, with a few methylenic units *n*, produces only the *syn* conformers and bent structures and makes the systems less flexible than monothiolate ones. More rigid systems could decrease the conformational mobility of the intermediates providing different reactivity.

Recent studies have discussed the preparation of homodinuclear and tetranuclear rhodium(I) complexes with alkyl dithiolate bridging ligands $[Rh_2(\mu\text{-}S(CH_2)_nS)(COD)_2]_x$ ($x = 1$, $n = 2$ and 3; $x = 2$, $n = 4$),[10] and their catalytic activity in the hydroformylation of olefins has been investigated.[11] Alkyl dithiolates have considerable potential as bridging ligands for synthesizing hetero-bimetallic complexes, and this aspect has scarcely been studied.[12]

In this paper, we describe the preparation and X-ray determination of the first examples of hetero-bimetallic PtRh and PdRh complexes of general formula [(phosphine)M(μ-dithiolate)Rh(COD)]ClO_4 (COD = 1,5-cyclooctadiene). The synthesis has been performed by reaction between the corresponding mononuclear platinum or palladium dithiolate−phosphine complex and the rhodium mononuclear complex $[Rh(COD)_2]ClO_4$.

Heterobimetallic complexes [(phosphine)M(μ-dithiolate)Rh(COD)]ClO_4 are of interest because they can be modified in any of their three ligand positions: the dithiolate bridging and the different terminal positions of the two metals. It should be pointed out that new complexes can be easily prepared by controlling the synthesis of this type of hetero-bimetallic compounds. By combining the characteristics of the ligands, the properties of the whole complex may be tuned.

Experimental Section

All reactions were carried out under nitrogen atmosphere using Schlenk techniques. Solvents were dried by standard methods and distilled under nitrogen prior to use. Starting materials [Pt(EDT)$(PPh_3)_2$],[13a] [Pt(PDT)$(PPh_3)_2$],[13b] [Pt(BDT)$(PPh_3)_2$],[13c] [Pt(EDT)(dppb)],[13d] [Pt(PDT)(dppb)],[13d] [Pt(EDT)(dppp)],[13d] [Pt(PDT)(dppp)],[13d] [Pt(BDT)(dppb)],[13c] [Pt(BDT)(dppp)],[13c] [Pd(BDT)(dppb)],[13c] and [Pd(BDT)(dppp)][13c] were prepared using already described procedures. Complexes which had not been previously described, [Pd(EDT)(dppb)], [Pd(PDT)(dppb)], [Pd(EDT)(dppp)], and [Pd(PDT)(dppp)], were prepared by a similar method.[13] The ^1H and ^{31}P NMR spectra were recorded on a Varian Gemini 300 spectrometer. Chemical shifts are reported in parts per million relative to external standards (tetramethylsilane (TMS) for ^1H and H_3PO_4 for ^{31}P). Elemental analyses were carried out with a Carlo-Elba microanalyzer. Mass spectra were recorded on a V. G. Autospec spectrometer.

Safety Note. Initially, we attempted to prepare the complexes with the tetrafluoroborate counteranion, but because of the greater facility to crystallize with the perchlorate anion, the complexes were isolated as perchlorate salts. We worked with these complexes in a number of organic solvents without any incident, and as solids, they seem to be very stable to shock and heat. Nevertheless, due to the unpredictable behavior of perchlorate salts,[14] they should be handled with extreme care.

Perchlorate salts of metal complexes with organic ligands are potentially explosive. Only small amounts of material should be prepared, and these should be handled with great caution.

[$(L)_2$M(μ-dithiolate)Rh(COD)]ClO_4 (M = Pt, Pd; dithiolate = EDT, PDT, BDT; $(L)_2$ = $(PPh_3)_2$, dppb, dppp). General Procedure for 1−15. A stoichiometric amount of $[Rh(COD)_2]ClO_4$ was added to a solution of the corresponding mononuclear compound [M(dithiolate)$(L)_2$] in dichloromethane (5 mL approximately), and the mixture was stirred at room temperature for 30 min. The reaction was controlled by thin-layer chromatography (TLC). The orange and yellow solutions were concentrated to 2 mL approximately and the complexes were isolated as microcrystalline solids by adding cold *n*-hexane. Crystals of some of the compounds were obtained by slow diffusion of *n*-hexane into a dichloromethane solution of the complexes.

[$(PPh_3)_2$Pt(μ-EDT)Rh(COD)]ClO_4 (1). *cis*-[Pt(EDT)$(PPh_3)_2$] (0.0300 g, 0.0370 mmol) and $[Rh(COD)_2]ClO_4$ (0.0155 g, 0.0370 mmol), orange crystals, 87% yield. ^1H NMR ($CDCl_3$, at 20 °C): δ 4.54 (m, 2 H, −CH═, COD), 3.90 (m, 2 H, −CH═, COD), 2.40 (m, 2 H, $-CH_2-$, COD), 2.28 (m, 2 H, $-CH_2-$, COD), 2.09 (m, 4 H, $-CH_2-$, COD), 3.08 (m, 2 H, $-CH_2-$, EDT), 2.55 (m, 2 H, $-CH_2-$, EDT), 7.3−7.5 (m, 30 H, Ph, PPh_3). ^{31}P NMR ($CDCl_3$, at 20 °C): δ 15.98 ($J^1(^{195}Pt-^{31}P)$ = 3219.9 Hz). Anal. Calcd for $PtRhClS_2P_2O_4C_{46}H_{46}$: C, 49.18; H, 4.10; S, 5.70. Found: C, 49.02; H, 4.31; S, 5.56.

[$(PPh_3)_2$Pt(μ-PDT)Rh(COD)]ClO_4 (2). *cis*-[Pt(PDT)$(PPh_3)_2$] (0.0300 g, 0.0362 mmol) and $[Rh(COD)_2]ClO_4$ (0.0152 g, 0.0362 mmol), orange crystals, 77% yield. ^1H NMR ($CDCl_3$, at 20 °C): δ 4.49 (m, 2 H, −CH═, COD), 3.89 (m, 2 H, −CH═, COD), 2.45 (m, 2 H, $-CH_2-$, COD), 2.35 (m, 2 H, $-CH_2-$, COD), 2.05 (m, 4 H, $-CH_2-$, COD), 2.58 (m, 4 H, $-SCH_2-$, PDT), 2.15 (m, 2 H, $-CH_2-$, PDT), 7.3−7.5 (m, 30 H, Ph, PPh_3). ^{31}P NMR ($CDCl_3$, at 20 °C): δ 17.93 ($J^1(^{195}Pt-^{31}P)$ = 3108.8 Hz). Anal. Calcd for $PtRhClS_2P_2O_4C_{47}H_{48}\cdot{}^1/_2CH_2Cl_2$: C, 48.35; H, 4.15; S, 5.43. Found: C, 48.05; H, 4.16; S, 5.26.

[$(PPh_3)_2$Pt(μ-BDT)Rh(COD)]ClO_4 (3). *cis*-[Pt(BDT)$(PPh_3)_2$] (0.0300 g, 0.0358 mmol) and $[Rh(COD)_2]ClO_4$ (0.0150 g, 0.0358 mmol), yellow crystals, 74% yield. ^1H NMR ($CDCl_3$, at 20 °C): δ 4.16 (m, 2 H, −CH═, COD), 4.12 (m, 2 H, −CH═ COD), 2.65 (m, 2 H, $-CH_2-$, COD), 2.10−2.30 (m, 4 H, $-CH_2-$, COD), 1.98 (m, 2 H, $-CH_2-$, COD), 2.35 (m, 4 H, $-SCH_2-$, BDT), 1.40 (m, 4 H, $-CH_2-$, BDT), 7.2−7.6 (m, 30 H, Ph, PPh_3). ^{31}P NMR ($CDCl_3$, at 20 °C): δ 19.13 ($J^1(^{195}Pt-^{31}P)$ = 2915.2 Hz). Anal. Calcd for $PtRhClS_2P_2O_4C_{48}H_{50}\cdot{}^1/_2CH_2Cl_2$: C, 48.85; H, 4.27; S, 5.38. Found: C, 48.25; H, 4.18; S, 5.58.

[(dppb)Pt(μ-EDT)Rh(COD)]ClO_4 (4). *cis*-[Pt(EDT)(dppb)] (0.0300 g, 0.0420 mmol) and $[Rh(COD)_2]ClO_4$ (0.0176 g, 0.0420 mmol), yellow solid, 75% yield. ^1H NMR ($CDCl_3$, at 20 °C): δ 4.25 (m, 2 H, −CH═, COD), 3.22 (m, 2 H, −CH═, COD), 2.80 (m, 4 H, $-CH_2-$, COD), 1.85 (m, 2 H, $-CH_2-$, COD), 1.65 (m, 2 H, $-CH_2-$, COD), 2.81 (m, 2 H, $-CH_2-$, EDT), 2.52 (m, 2 H, $-CH_2-$, EDT), 7.75 (m, 10 H, Ph, dppb), 7.58 (m, 5 H, Ph, dppb), 7.51 (m, 5 H, Ph, dppb), 2.80 (m, 4 H, $-PCH_2-$, dppb), 2.12 (m, 4 H, $-CH_2-$, dppb). ^{31}P NMR ($CDCl_3$, at 20 °C): δ 15.33 ($J^1(^{195}Pt-^{31}P)$ = 3127.9 Hz). FAB: *m/z* 924 [M − $ClO_4]^+$. Anal. Calcd for $PtRhClS_2P_2O_4C_{38}H_{40}\cdot{}^1/_2CH_2Cl_2$: C, 43.38; H, 4.22; S, 6.04. Found: C, 43.15; H, 4.22; S, 5.90.

[(dppb)Pt(μ-PDT)Rh(COD)]ClO_4 (5). *cis*-[Pt(PDT)(dppb)] (0.0300 g, 0.0412 mmol) and $[Rh(COD)_2]ClO_4$ (0.0173 g, 0.0412 mmol), orange solid, 69% yield. ^1H NMR ($CDCl_3$, at 20 °C): δ 4.30 (m, 2 H, −CH═,

(8) Capdevila, M.; Clegg, W.; González-Duarte, P.; Jarid, A.; Lledós, A. *Inorg. Chem.* **1996**, *35*, 490.
(9) (a) Bonnet, J.-J.; Kalck, P.; Poilblanc, R. *Inorg. Chem.* **1977**, *16*, 1514. (b) Bonnet, J.-J.; Thorez, A.; Maisonnat, A.; Galy, J.; Poilblanc, R. *J. Am. Chem. Soc.* **1979**, *101*, 5940. (c) Usón, R.; Oro, L. A.; Ciriano, M. A.; Pinillos, M. T.; Tiripicchio, A.; Tiripicchio-Camellini, M. *J. Organomet. Chem.* **1981**, *205*, 247.
(10) Masdeu, A. M.; Ruiz, A.; Castillón, S.; Claver, C.; Hitchcock, P. B.; Chaloner, P. A.; Bó, C.; Poblet, J. M.; Sarasa, P. *J. Chem. Soc., Dalton Trans.* **1993**, 2689.
(11) Aaliti, A.; Masdeu, A. M.; Ruiz, A.; Claver, C. *J. Organomet. Chem.* **1995**, *489*, 101.
(12) Aggarwal, R. C.; Mitra, R. *Ind. J. Chem.*, A **1994**, *33*, 55.
(13) (a) Rauchfuss, T. B.; Roundhill, D. M. *J. Am. Chem. Soc.* **1975**, *97*, 3386. (b) Rauchfuss, T. B.; Shu, J. S.; Roundhill, D. M. *Inorg. Chem.* **1976**, *15*, 2096. (c) Forniés-Cámer, J.; Aaliti, A.; Ruiz, N.; Masdeu-Bultó, A. M.; Claver, C.; Cardin, C. J. *J. Organomet. Chem.*, in press. (d) Fazlur-Rahnam, A. K.; Verkade, J. G. *Inorg. Chem.* **1992**, *31*, 969.
(14) (a) Everett, K.; Graf, F. A., Jr. In *CRC Handbook of Laboratory Safety*, 2nd ed.; Steere, N. V., Ed.; Chemical Rubber Co.: Cleveland, OH, 1971. (b) Wolsey, W. C. *J. Chem. Educ.* **1973**, *50*, A335. (c) Raymond, K. N. *Chem. Eng. News* **1983**, *61* (Dec 5), 4.

COD), 3.30 (m, 2 H, −CH═, COD), 2.25 (m, 4 H, $-CH_2-$, COD), 1.95 (m, 2 H, $-CH_2-$, COD), 1.72 (m, 2 H, $-CH_2-$, COD), 2.90 (m, 4 H, $-SCH_2-$, PDT), 2.40 (m, 2 H, $-CH_2-$, PDT), 7.80 (m, 5 H, Ph, dppb), 7.72 (m, 5 H, Ph, dppb), 7.51 (m, 10 H, Ph, dppb), 2.85 (m, 4 H, $-PCH_2-$, dppb), 2.15 (m, 4 H, $-CH_2-$, dppb). ^{31}P NMR ($CDCl_3$, at 20 °C): δ 16.19 ($J^1(^{195}Pt-^{31}P) = 3035.8$ Hz). FAB: *m/z* 938 [M − ClO_4]$^+$. Anal. Calcd for $PtRhClS_2P_2O_4C_{39}H_{42}\cdot{}^1/_2CH_2Cl_2$: C, 43.93; H, 4.35; S, 5.94. Found: C, 43.82; H, 4.31; S, 6.24.

[(dppb)Pt(μ-BDT)Rh(COD)]ClO_4 (6). *cis*-[Pt(BDT)(dppb)] (0.0300 g, 0.0405 mmol) and $[Rh(COD)_2]ClO_4$ (0.0170 g, 0.0405 mmol), yellow crystals, 74% yield. ^{1}H NMR ($CDCl_3$, at 20 °C): δ 4.12 (m, 4 H, −CH═, COD), 2.30 (m, 4 H, $-CH_2-$, COD), 2.15 (m, 2 H, $-CH_2-$, COD), 2.00 (m, 2 H, $-CH_2-$, COD), 3.28 (m, 2 H, $-SCH_2-$, BDT), 2.80 (m, 2 H, $-SCH_2-$, BDT), 1.80 (m, 4 H, $-CH_2-$, BDT), 8.20 (m, 5 H, Ph, dppb), 7.40−7.70 (m, 15 H, Ph, dppb), 2.55 (m, 4 H, $-PCH_2-$, dppb), 1.70 (m, 4 H, $-CH_2-$, dppb). ^{31}P NMR ($CDCl_3$, at 20 °C): δ 17.69 ($J^1(^{195}Pt-^{31}P) = 2909.9$ Hz). Anal. Calcd for $PtRhClS_2P_2O_4C_{40}H_{44}\cdot{}^1/_2CH_2Cl_2$: C, 44.45; H, 4.47; S, 5.86. Found: C, 44.20; H, 4.65; S, 5.96.

[(dppp)Pt(μ-EDT)Rh(COD)]ClO_4 (7). *cis*-[Pt(EDT)(dppp)] (0.0300 g, 0.0427 mmol) and $[Rh(COD)_2]ClO_4$ (0.0179 g, 0.0427 mmol), yellow solid, 72% yield. ^{1}H NMR ($CDCl_3$, at 20 °C): δ 4.25 (m, 2 H, −CH═, COD), 3.12 (m, 2 H, −CH═, COD), 2.80 (m, 4 H, $-CH_2-$, COD), 1.92 (m, 2 H, $-CH_2-$, COD), 1.75 (m, 2 H, $-CH_2-$, COD), 3.20 (m, 2 H, $-CH_2-$, EDT), 2.55 (m, 2 H, $-CH_2-$, EDT), 7.82 (m, 5 H, Ph, dppp), 7.70 (m, 5 H, Ph, dppp), 7.52 (m, 5 H, Ph, dppp), 7.41 (m, 5 H, Ph, dppp), 2.80 (m, 4 H, $-PCH_2-$, dppp), 2.15 (m, 2 H, $-CH_2-$, dppp). ^{31}P NMR ($CDCl_3$, at 20 °C): δ 0.01 ($J^1(^{195}Pt-^{31}P) = 3004.5$ Hz). FAB: *m/z* 910 [M − ClO_4]$^+$. Anal. Calcd for $PtRhClS_2P_2O_4C_{37}H_{38}\cdot{}^1/_2CH_2Cl_2$: C, 42.81; H, 4.08; S, 6.09. Found: C, 42.49; H, 4.06; S, 6.12.

[(dppp)Pt(μ-PDT)Rh(COD)]ClO_4 (8). *cis*-[Pt(PDT)(dppp)] (0.0300 g, 0.0420 mmol) and $[Rh(COD)_2]ClO_4$ (0.0176 g, 0.0420 mmol), orange solid, 81% yield. ^{1}H NMR ($CDCl_3$, at 20 °C): δ 4.40 (m, 2 H, −CH═, COD), 3.60 (m, 2 H, −CH═, COD), 3.15 (m, 4 H, $-CH_2-$, COD), 2.01 (m, 2 H, $-CH_2-$, COD), 1.35 (m, 2 H, $-CH_2-$, COD), 2.85 (m, 4 H, $-SCH_2-$, PDT), 2.35 (m, 2 H, $-CH_2-$, PDT), 7.85 (m, 5 H, Ph, dppp), 7.70 (m, 5 H, Ph, dppp), 7.50 (m, 10 H, Ph, dppp), 2.31 (m, 4 H, $-PCH_2-$, dppp), 2.01 (m, 2 H, $-CH_2-$, dppp). ^{31}P NMR ($CDCl_3$, at 20 °C): δ 0.60 ($J^1(^{195}Pt-^{31}P) = 2919.4$ Hz). FAB: *m/z* 924 [M − ClO_4]$^+$. Anal. Calcd for $PtRhClS_2P_2O_4C_{38}H_{40}\cdot{}^1/_2CH_2Cl_2$: C, 42.25; H, 4.14; S, 5.78. Found: C, 42.18; H, 4.03; S, 5.76.

[(dppp)Pt(μ-BDT)Rh(COD)]ClO_4 (9). *cis*-[Pt(BDT)(dppp)] (0.0300 g, 0.0412 mmol) and $[Rh(COD)_2]ClO_4$ (0.0173 g, 0.0412 mmol), yellow crystals, 70% yield. ^{1}H NMR ($CDCl_3$, at 20 °C): δ 4.21 (m, 4 H, −CH═, COD), 2.55 (m, 4 H, $-CH_2-$, COD), 2.32 (m, 2 H, $-CH_2-$, COD), 1.95 (m, 2 H, $-CH_2-$, COD), 2.80 (m, 4 H, $-SCH_2-$, BDT), 1.95 (m, 4 H, $-CH_2-$, BDT), 8.20 (m, 5 H, Ph, dppp), 7.70−7.40 (m, 15 H, Ph, dppp), 2.12 (m, 4 H, $-PCH_2-$, dppp), 1.92 (m, 2 H, $-CH_2-$, dppp). ^{31}P NMR ($CDCl_3$, at 20 °C): δ 1.14 ($J^1(^{195}Pt-^{31}P) = 2785.7$ Hz). Anal. Calcd for $PtRhClS_2P_2O_4C_{39}H_{42}\cdot{}^1/_2CH_2Cl_2$: C, 44.04; H, 4.36; S, 5.95. Found: C, 44.01; H, 4.50; S, 6.04.

[(dppb)Pd(μ-EDT)Rh(COD)]ClO_4 (10). *cis*-[Pd(EDT)(dppb)] (0.0300 g, 0.0478 mmol) and $[Rh(COD)_2]ClO_4$ (0.0201 g, 0.0478 mmol), orange solid, 70% yield. ^{1}H NMR ($CDCl_3$, at 20 °C): δ 4.28 (m, 2 H, −CH═, COD), 3.12 (m, 2 H, −CH═, COD), 3.00 (m, 4 H, $-CH_2-$, COD), 1.85 (m, 2 H, $-CH_2-$, COD), 1.62 (m, 2 H, $-CH_2-$, COD), 2.80 (m, 2 H, $-CH_2-$, EDT), 2.60 (m, 2 H, $-CH_2-$, EDT), 7.72 (m, 10 H, Ph, dppb), 7.60 (m, 5 H, Ph, dppb), 7.51 (m, 5 H, Ph, dppb), 2.60 (m, 4 H, $-PCH_2-$, dppb), 2.12 (m, 4 H, $-CH_2-$, dppb). ^{31}P NMR ($CDCl_3$, at 20 °C): δ 25.68. FAB: *m/z* 835 [M − ClO_4]$^+$. Anal. Calcd for $PdRhClS_2P_2O_4C_{38}H_{40}\cdot CH_2Cl_2$: C, 45.93; H, 4.51; S, 6.29. Found: C, 45.48; H, 4.51; S, 6.32.

[(dppb)Pd(μ-PDT)Rh(COD)]ClO_4 (11). *cis*-[Pd(PDT)(dppb)] (0.0300 g, 0.0470 mmol) and $[Rh(COD)_2]ClO_4$ (0.0197 g, 0.0470 mmol), orange solid, 74% yield. ^{1}H NMR ($CDCl_3$, at 20 °C): δ 4.30 (m, 2 H, −CH═, COD), 3.30 (m, 2 H, −CH═, COD), 2.2−1.7 (m, 8 H, $-CH_2-$, COD), 2.82 (m, 4 H, $-SCH_2-$, PDT), 2.0−2.2 (m, 2 H, $-CH_2-$, PDT), 7.74 (m, 5 H, Ph, dppb), 7.60 (m, 5 H, Ph, dppb), 7.55 (m, 10 H, Ph, dppb), 2.70 (m, 4 H, $-PCH_2-$, dppb), 2.0−2.2 (m, 4 H, $-CH_2-$, dppb). ^{31}P NMR ($CDCl_3$, at 20 °C): δ 25.59. FAB: *m/z* 849 [M − ClO_4], 741 [M − COD − ClO_4], 423 [M − dppb − ClO_4]. Anal. Calcd for $PdRhClS_2P_2O_4C_{39}H_{42}\cdot CH_2Cl_2$: C, 46.47; H, 4.64; S, 6.20. Found: C, 46.12; H, 4.62; S, 6.22.

[(dppb)Pd(μ-BDT)Rh(COD)]ClO_4 (12). *cis*-[Pd(BDT)(dppb)] (0.0300 g, 0.0460 mmol) and $[Rh(COD)_2]ClO_4$ (0.0193 g, 0.0460 mmol), red cyrstals, 69% yield. ^{1}H NMR ($CDCl_3$, at 20 °C): δ 4.19 (m, 2 H, −CH═, COD), 3.99 (m, 2 H, −CH═, COD), 2.29 (m, 4 H, $-CH_2-$, COD), 2.12 (m, 2 H, $-CH_2-$, COD), 2.02 (m, 2 H, $-CH_2-$, COD), 3.38 (m, 2 H, $-SCH_2-$, BDT), 2.62 (m, 2 H, $-SCH_2-$, BDT), 1.90 (m, 2 H, $-CH_2-$, BDT), 1.62 (m, 2 H, $-CH_2-$, BDT), 8.20 (m, 5 H, Ph, dppb), 7.4−7.8 (m, 15 H, Ph, dppb), 2.53 (m, 4 H, $-PCH_2-$, dppb), 1.70 (m, 4 H, $-CH_2-$, dppb). ^{31}P NMR ($CDCl_3$, at 20 °C): δ 26.89. Anal. Calcd for $PdRhClS_2P_2O_4C_{39}H_{42}$: C, 48.37; H, 4.97; S, 6.37. Found: C, 48.06; H, 5.05; S, 6.32.

[(dppp)Pd(μ-EDT)Rh(COD)]ClO_4 (13). *cis*-[Pd(EDT)(dppp)] (0.0300 g, 0.0491 mmol) and $[Rh(COD)_2]ClO_4$ (0.0206 g, 0.0491 mmol), orange solid, 84% yield. ^{1}H NMR ($CDCl_3$, at 20 °C): δ 4.30 (m, 2 H, −CH═, COD), 3.15 (m, 2 H, −CH═, COD), 3.00 (m, 4 H, $-CH_2-$, COD), 1.95 (m, 2 H, $-CH_2-$, COD), 1.75 (m, 2 H, $-CH_2-$, COD), 3.15 (m, 2 H, $-CH_2-$, EDT), 2.65 (m, 2 H, $-CH_2-$, EDT), 7.72 (m, 10 H, Ph, dppp), 7.52 (m, 5 H, Ph, dppp), 7.47 (m, 5 H, Ph, dppp), 2.65 (m, 4 H, $-PCH_2-$, dppp), 2.15 (m, 2 H, $-CH_2-$, dppp). ^{31}P NMR ($CDCl_3$, at 20 °C): δ 9.94. FAB: *m/z* 821 [M − ClO_4]$^+$. Anal. Calcd for $PdRhClS_2P_2O_4C_{37}H_{38}\cdot{}^1/_2CH_2Cl_2$: C, 46.60; H, 4.34; S, 6.63. Found: C, 46.28; H, 4.40; S, 6.63.

[(dppp)Pd(μ-PDT)Rh(COD)]ClO_4 (14). *cis*-[Pd(PDT)(dppp)] (0.0300 g, 0.0478 mmol) and $[Rh(COD)_2]ClO_4$ (0.0201 g, 0.0478 mmol), orange solid, 77% yield. ^{1}H NMR ($CDCl_3$, at 20 °C): δ 4.40 (m, 2 H, −CH═, COD), 3.60 (m, 2 H, −CH═, COD), 3.20 (m, 4 H, $-CH_2-$, COD), 1.85 (m, 2 H, $-CH_2-$, COD), 1.40 (m, 2 H, $-CH_2-$, COD), 2.70 (m, 4 H, $-SCH_2-$, PDT), 2.30 (m, 2 H, $-CH_2-$, PDT), 7.85 (m, 5 H, Ph, dppp), 7.65 (m, 5 H, Ph, dppp), 7.45 (m, 10 H, Ph, dppp), 2.30 (m, 4 H, $-PCH_2-$, dppp), 2.05 (m, 2 H, $-CH_2-$, dppp). ^{31}P NMR ($CDCl_3$, at 20 °C): δ 8.70. FAB: *m/z* 835 [M − ClO_4]$^+$. Anal. Calcd for $PdRhClS_2P_2O_4C_{38}H_{40}\cdot CH_2Cl_2$: C, 45.93; H, 4.51; S, 6.29. Found: C, 45.96; H, 4.48; S, 6.27.

[(dppp)Pd(μ-BDT)Rh(COD)]ClO_4 (15). *cis*-[Pd(BDT)(dppp)] (0.0300 g, 0.0470 mmol) and $[Rh(COD)_2]ClO_4$ (0.0197 g, 0.0470 mmol), orange solid, 66% yield. ^{1}H NMR ($CDCl_3$, at 20 °C): δ 4.27 (m, 2 H, −CH═, COD), 4.09 (m, 2 H, −CH═, COD), 2.57 (m, 4 H, $-CH_2-$, COD), 2.32 (m, 2 H, $-CH_2-$, COD), 2.02 (m, 2 H, $-CH_2-$, COD), 3.07 (pt, 4 H, $-SCH_2-$, BDT), 1.85 (m, 4 H, $-CH_2-$, BDT), 8.15 (m, 5 H, Ph, dppp), 7.2−7.7 (m, 15 H, Ph, dppp), 2.17 (m, 4 H, $-PCH_2-$, dppp), 2.02 (m, 2 H, $-CH_2-$, dppp). ^{31}P NMR ($CDCl_3$, at 20 °C): δ 9.38. FAB: *m/z* 850 [MH − ClO_4]$^+$. Anal. Calcd for $PdRhClS_2P_2O_4C_{39}H_{42}\cdot CH_2Cl_2$: C, 46.46; H, 4.64; S, 6.20. Found: C, 46.26; H, 4.72; S, 6.32.

Crystal Data for the Compounds 1−3, 6, 9, and 12. Suitable crystals of the complexes **1**−**3**, **6**, **9**, and **12** were grown by diffusing *n*-hexane into a solution of the above compounds in dichloromethane and mounted on a glass fiber. The data were collected and processed at room temperature on a Mar Research image plate scanner, graphite-monochromated Mo Kα radiation was used to measure 95/2° frames, 180 s per frame in all cases, except for compound **3** where 1200 s exposure was used.

Compound **1**: $PtRhClS_2P_2O_6C_{46}H_{46}$, $M = 1154.34$, triclinic, $a = 11.311(6)$ Å, $b = 12.991(6)$ Å, $c = 16.140(6)$ Å, $\alpha = 84.85(6)°$, $\beta = 75.73(6)°$, $\gamma = 86.43(6)°$, $V = 2287.2$ Å^3, space group $P\bar{1}$ (No. 2), $Z = 2$, $D_c = 1.676$ g·cm^{-3}, $F(000) = 1144$. Orange, crystal dimensions 0.15 × 0.22 × 0.17 mm, μ(Mo Kα) = 36.82 cm^{-1}.

Compound **2**: $PtRhCl_2S_2P_2O_5C_{47.5}H_{48}$, $M = 1193.82$, triclinic, $a = 11.084(5)$ Å, $b = 13.094(6)$ Å, $c = 16.338(6)$ Å, $\alpha = 86.06(6)°$, $\beta = 75.67(6)°$, $\gamma = 88.55(6)°$, $V = 2291.9$ Å^3, space group $P\bar{1}$ (No. 2), $Z = 2$, $D_c = 1.730$ g·cm^{-3}, $F(000) = 1184$. Orange, crystal dimensions 0.34 × 0.26 × 0.20 mm, μ(Mo Kα) = 37.32 cm^{-1}.

Compound **3**: $PtRhCl_2S_2P_2O_4C_{48.5}H_{42}$, $M = 1184.79$, orthorhombic, $a = 14.439(6)$ Å, $b = 19.807(6)$ Å, $c = 38.156(6)$ Å, $V = 10912.4$ Å^3, space group *Pbca* (No. 61), $Z = 8$, $D_c = 1.442$ g·cm^{-3}, $F(000) = 4680$. Yellow, crystal dimensions 0.43 × 0.20 × 0.24 mm, μ(Mo Kα) = 31.34 cm^{-1}.

Table 1. Crystal Data for Compounds **1**−**3**, **6**, **9**, and **12**

	1	**2**	**3**	**6**	**9**	**12**
formula	$PtRhClS_2P_2O_4C_{46}H_{46}$	$PtRhClS_2P_2O_4C_{47}H_{48}$	$PtRhClS_2P_2O_4C_{48}H_{42}$	$PtRhClS_2P_2O_4C_{40}H_{48}$	$PtRhClS_2P_2O_4C_{39}H_{38}$	$PdRhClS_2P_2O_4C_{40}H_{48}$
solvent	$2H_2O$	$^1/_2CH_2Cl_2 \cdot H_2O$	$^1/_2CH_2Cl_2$	$^1/_2CH_2Cl_2$	$^1/_2CH_2Cl_2$	$^1/_2CH_2Cl_2$
fw, g·mol^{-1}	1154.34	1193.82	1184.79	1093.75	1070.65	1005.06
space group	$P\bar{1}$	$P\bar{1}$	Pbca	$P2_1/c$	$P2_1/c$	$P2_1/c$
temp, °C	20	20	20	20	20	20
a, Å	11.311(6)	11.084(5)	14.439(6)	20.338(6)	20.326(6)	20.365(6)
b, Å	12.991(6)	13.094(6)	19.807(6)	14.227(6)	14.109(6)	14.186(6)
c, Å	16.140(6)	16.338(6)	38.156(6)	14.570(6)	14.368(6)	14.592(6)
α, deg	84.86(6)	86.06(6)				
β, deg	75.73(6)	75.67(6)		100.94(6)	100.90(6)	101.04(6)
γ, deg	86.43(6)	88.55(6)				
V, Å^3	2287.2	2291.9	10912.4	4139.1	4046.2	4137.6
Z	2	2	8	4	4	4
λ(Mo Kα) Å	0.710 73	0.710 73	0.710 73	0.710 73	0.710 73	0.710 73
ρ(calcd), g·cm^{-3}	1.676	1.730	1.442	1.755	1.758	1.613
μ(Mo Kα), cm^{-1}	36.82	37.32	31.34	41.22	42.15	11.81
R_1[a]	0.0427	0.0470	0.0864	0.0536	0.0380	0.0507
R_{w2}[b]	0.1151	0.1264	0.2457	0.1449	0.0990	0.1500

[a] $R_1 = \sum||F_o| - |F_c||/\sum|F_o|$. [b] $R_{w2} = [\sum w(F_o^2 - F_c^2)/\sum w(F_o^2)^2]^{1/2}$; $w = 1/[\sigma^2(F_o^2) + (0.1025P)^2 + 21.43P]$, where $P = (\max(F_o^2,0) + 2F_c^2)/3)$.

Compound **6**: $PtRhCl_2S_2P_2O_4C_{40.5}H_{48}$, $M = 1093.75$, monoclinic, $a = 20.338(6)$ Å, $b = 14.227(6)$ Å, $c = 14.570(6)$ Å, $\beta = 100.94(6)°$, $V = 4139.1$ Å^3, space group $P2_1/c$ (No. 14), $Z = 4$, $D_c = 1.755$ g·cm^{-3}, $F(000) = 2168$. Yellow, crystal dimensions 0.21 × 0.29 × 0.22 mm, μ(Mo Kα) = 41.22 cm^{-1}.

Compound **9**: $PtRhCl_2S_2P_2O_4C_{39.5}H_{38}$, $M = 1070.65$, monoclinic, $a = 20.326(6)$ Å, $b = 14.109(6)$ Å, $c = 14.368(6)$ Å, $\beta = 100.90(6)°$, $V = 4046.2$ Å^3, space group $P2_1/c$ (No. 14), $Z = 4$, $D_c = 1.758$ g·cm^{-3}, $F(000) = 2100$. Yellow, crystal dimensions 0.24 × 0.32 × 0.26 mm, μ(Mo Kα) = 42.15 cm^{-1}.

Compound **12**: $PdRhCl_2S_2P_2O_6C_{40.5}H_{48}$, $M = 1005.06$, monoclinic, $a = 20.365(6)$ Å, $b = 14.186(6)$ Å, $c = 14.592(6)$ Å, $\beta = 101.04(6)°$, $V = 4137.6$ Å^3, space group $P2_1/c$ (No. 14), $Z = 4$, $D_c = 1.613$ g·cm^{-3}, $F(000) = 2040$. Dark red, crystal dimensions 0.17 × 0.22 × 0.24 mm, μ(Mo Kα) = 11.81 cm^{-1}.

The XDS[15] package was used to give the following: 7052 unique reflections [merging $R = 0.0280$] (**1**), 6888 [merging $R = 0.0281$] (**2**), 9013 [merging $R = 0.1360$] (**3**), 5588 [merging $R = 0.0380$] (**6**), 6486 [merging $R = 0.0374$] (**9**), 5708 [merging $R = 0.0494$] (**12**).

The heavy atoms were found from the Patterson map using the SHELX86[16] program and refined subsequently from successive difference Fourier maps using SHELXL93[17] by full-matrix least squares of 553 (**1**), 579 (**2**), 319 (**3**), 511 (**6**), 501 (**9**), and 511 (**12**) variables, to a final R-factor of 0.043 (**1**), 0.047 (**2**), 0.086 (**3**), 0.054 (**6**), 0.038 (**9**), and 0.051 (**12**) for 6332 (**1**), 6239 (**2**), 2120 (**3**), 4614 (**6**), 5343 (**9**), 4452 (**12**) reflections with $[F_o] > 4\sigma(F_o)$. All atoms were revealed by the Fourier map difference. Non-hydrogen atoms were refined anisotropically (except the C atoms of the phenyl groups of the PPh_3 ligand in complex **3**, which were fixed by using a riding model in which the C−C vector is fixed at 1.39 Å). A disorder produced by the motion of the central methylenic C atoms in the BDT ligand can be seen in **3** and **6**. In all cases, a disorder was found in ClO_4^- anion. Hydrogen atoms were placed geometrically and then refined with fixed isotropic atomic displacement parameters. The weighting scheme $w = 1/[\sigma^2(F_o^2) + (aP)^2 + bP]$, where $P = (\max(F_o^2,0) + 2F_c^2)/3$, $a = 0.0742$ (**1**), 0.0900 (**2**), 0.1577 (**3**), 0.1072 (**6**), 0.0621 (**9**), 0.1209 (**15**) and $b = 9.84$ (**1**), 9.39 (**2**), 139.81 (**3**), 15.24 (**6**), 7.18 (**9**), 4.50 (**12**) with $\sigma(F_o)$ from counting statistics, gave satisfactory agreement analyses. Data collection parameters including R ($[F_o] > 4\sigma(F_o)$) and R' (all data) values are summarized in Table 1.

(15) Kabsch, W. *J. Appl. Crystallogr.* **1993**, *26*, 795.
(16) Sheldrick, G. M. *SHELXS-86: Program for Crystal Structure Solutions;* University of Göttingen: Göttingen, Germany, 1986.
(17) Sheldrick, G. M. *SHELXS-93: Program for Crystal Structure Solutions;* University of Göttingen: Göttingen, Germany, 1993.

Results and Discussion

The best method for preparing hetero-bimetallic complexes M_1-M_1' has been shown to be the direct reaction between the two mononuclear fragments $M_1 + M_1'$.[1] Another possible method described in the literature is the reaction between the corresponding homo-dinuclear monothiolates $M_2 + M_2'$, but, in these cases, yields were poor.[7b] The $M_1 + M_1'$ synthesis can be tackled in two ways, depending on which of the mononuclear fragments (M_1 or M_1') contains the coordinated dithiolate ligand. The syntheses described in this paper require the mononuclear platinum or palladium dithiolate complexes to be used because rhodium ones stabilize the dinuclear species $[L_2Rh(\mu\text{-dithiolate})RhL_2]$.[10]

Previous studies[13] reported the preparation of mononuclear platinum and palladium complexes containing coordinated dithiolates with the general formula of [M(dithiolate)(P−P)] (M = Pt, Pd; dithiolate = EDT^{2-} (1,2-ethanedithiolate), PDT^{2-} (1,3-propanedithiolate), BDT^{2-} (1,4-buthanedithiolate); P−P = $(PPh_3)_2$, dppb (1,4-bis(diphenylphosphino)butane), and dppp (1,3-bis(diphenylphosphino)propane)). Due to the presence of the dithiolate nonbonding electrons, these complexes may be expected to coordinate to a second metal. With the aim of developing the potential of this species as metalloligands in the synthesis of hetero-bimetallic complexes, we studied their reactivity with the mononuclear complex $[Rh(COD)_2]ClO_4$, in which it is known that one diolefin can be easily displaced.

Reaction between a dichloromethane solution of complex $[Pt(S(CH_2)_2S)(PPh_3)_2]$ with the rhodium complex $[Rh(COD)_2]ClO_4$ at room temperature for 30 min leads to the formation of an orange compound which is isolated in high yield (87%) by adding hexane and characterized as the new hetero-binuclear complex **1**, $[(PPh_3)_2Pt(\mu\text{-}S(CH_2)_2S)Rh(COD)]ClO_4$ (reaction 1).

$$[Pt(EDT)(PPh_3)_2] + [Rh(COD)_2]ClO_4 \rightarrow \underset{\mathbf{1}}{[(PPh_3)_2Pt(\mu\text{-EDT})Rh(COD)]ClO_4} + COD \quad (1)$$

This reaction was highly selective in the formation of hetero-bimetallic compound **1**. Other species were not observed either in solid state or in solution. This method was extended to a series of several dithiolates and diphosphines (Scheme 1), and in all cases the desired hetero-bimetallic complexes were

Scheme 1

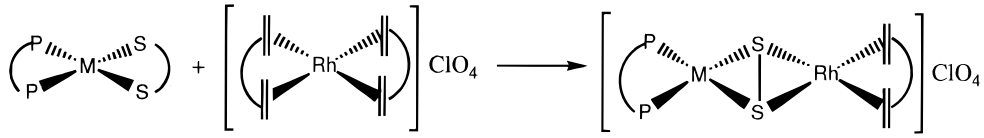

[(P-P)M(μ-S-S)Rh(COD)]ClO_4

M = Pt, P-P = $(PPh_3)_2$, S-S = EDT (**1**), PDT (**2**), BDT (**3**);

M = Pt, P-P = dppb, S-S = EDT (**4**), PDT (**5**), BDT (**6**);

M = Pt, P-P = dppp, S-S = EDT (**7**), PDT (**8**), BDT (**9**);

M = Pd, P-P = dppb, S-S = EDT (**10**), PDT (**11**), BDT (**12**);

M = Pd, P-P = dppp, S-S = EDT (**13**), PDT (**14**), BDT (**15**);

Table 2. $^{31}P\{^1H\}$ NMR Spectra (δ, ppm) for Complexes **1**−**15** in $CDCl_3$ Solutions with H_3PO_4 as External Standard

complex	δ, ppm	^1J, Hz	complex	δ, ppm	^1J, Hz
1	15.98	3219.9	**9**	1.14	2785.7
2	17.93	3108.8	**10**	25.68	
3	19.13	2915.2	**11**	25.59	
4	15.33	3127.9	**12**	26.89	
5	16.19	3035.8	**13**	9.94	
6	17.69	2909.9	**14**	8.70	
7	0.01	3004.5	**15**	9.38	
8	0.60	2919.4			

obtained in high yields. Therefore, it is an efficient way for the preparation of hetero-bimetallic complexes which can be generalized.

The hetero-binuclear nature of these species in the solid state was shown by X-ray structural analysis for the complexes **1**−**3**, **6**, **9**, and **12**. FAB mass spectra of complexes **4**, **5**, **7**, **8**, **10**, and **11** had a signal at *m/z* which corresponded to the cationic species $[(P-P)M(\mu\text{-dithiolate})Rh(COD)]^+$.

NMR Spectroscopic Characterization. The spectroscopic data (^1H NMR in the experimental section and $^{31}P\{^1H\}$ NMR in Table 2) show that there are no redistribution reactions in solution. The $^{31}P\{^1H\}$ NMR spectra show only one signal in all of the complexes, as expected for equivalent phosphorus atoms. In the case of platinum compounds the satellites attributed to the $^{31}P-^{195}Pt$ coupling corresponding to the coordinated phosphine were observed. The palladium complexes show the singlet that is to be expected when the diphosphine ligand coordinates to the palladium center.

As far as the $^{31}P\{^1H\}$ data for all of the complexes are concerned, the influence of the diphosphine ring size on the ^{31}P displacement previously reported for other diphosphine complexes[18] can be seen by comparing dppb and dppp complexes. The dithiolate ring size has less influence on the ^{31}P signals, which was also the case in related mononuclear platinum dithiolate complexes.[13]

For the platinum complexes **1**−**9**, the coupling constants $^1J(Pt-P)$ have higher values in the hetero-bimetallic complexes than in the mononuclear ones[13] (for example, $^1J(Pt-P)$ is 3219.9 Hz for complex **1** and 2884 Hz for complex $[Pt(S(CH_2)_2S)(PPh_3)_2]$), which indicates that the M−P bond strengthens. This, in turn, can be related to the weakening of the M−S bond due to bridge coordination.

The signals of the ^1H NMR spectra were assigned by correlation of $^1H-^1H$ COSY experiments due to the overlap of the signals in the methylenic region. One example of the COSY experiment for complex **1** is shown in Figure 1.

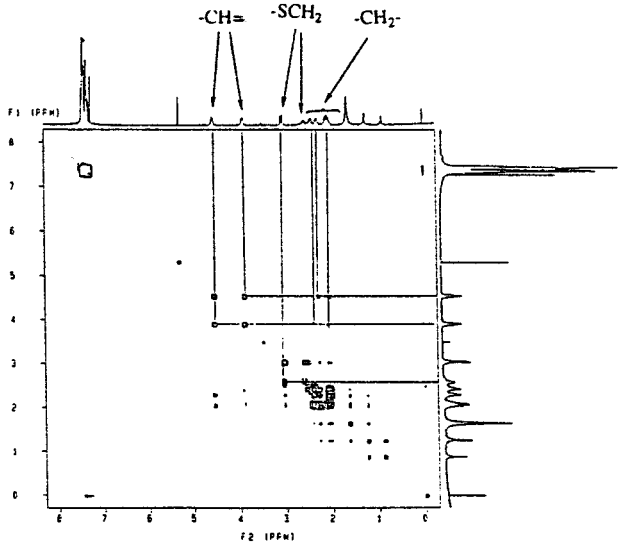

Figure 1. COSY experiment for complex **1**.

In the complexes **1**−**5**, **7**, **8**, and **10**−**15**, the olefinic protons corresponding to the coordinated COD appear in the ^1H NMR spectra as two multiplet signals, as expected for a bent structure with a different environment for each of the two different faces of the coordination plane.[10] However, in the BDT complexes **6** and **9** these signals are not resolved and appear as a broad signal. Because of the bent structure and the *endo*- and *exo*-positions of methylenic COD protons, four non-equivalent sites should be expected for methylenic COD protons. However, all of the non-equivalencies are not resolved, and the spectra show only three signals for all of the complexes **1**−**15** (except for complex **11** for which a broad signal is observed).

As far as the dithiolate protons for complex **1** and the rest of the complexes with EDT^{2-} (**4**, **7**, **10**, and **13**) are concerned, the resonances attributed to the methylenic groups of the dithiolate bridging ligands, which should be equivalent in a homometallic environment, clearly split into two signals around 3.0 and 2.5 ppm. One of the signals may correspond to the protons oriented to the platinum or palladium center and the other to the rhodium center. This behavior is not observed for the complexes with the PDT^{2-} and BDT^{2-} in which broad signals were detected, probably due to conformational exchange of the condensed six- and seven-membered metalocycles formed by coordination to both metals.

In order to determine which of the methylenic signals of the 1,2-ethanodithiolate correspond to the protons oriented to the rhodium or platinum center, NOE experiments were performed for complex **1**. The more significative NOE effect values and the proposed assignation of methylenic and olefinic signals for

(18) Garrou, P. E. *Chem. Rev.* **1981**, *81*, 229.

Scheme 2

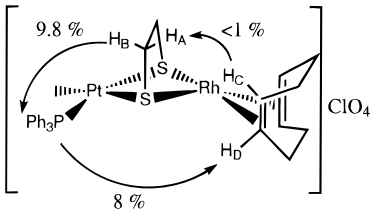

Scheme 3

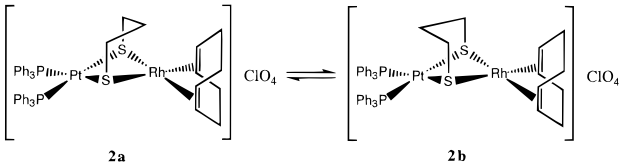

2a **2b**

complex **1** are shown in Scheme 2. Irradiation of the H_A dithiolate proton is not conclusive because it produces a similar NOE effect (0.8%) on the aromatic and olefinic protons. However, when H_B was irradiated, aromatic PPh_3 signals show enhancement of 9.8% and no NOE effect was observed on the olefinic protons H_C and H_D. This suggests that H_B protons may be oriented to the platinum center that contains the phosphine ligands and H_A protons to the rhodium center. The inverse experiments supported these results.

The ^1H NMR spectra for complex **1** was unaltered in the temperature range from +60 to −90 °C.

In the case of PDT^{2-} complex **2**, since the methylenic COD protons appear as two broad signals, in the ^1H NMR spectrum at room temperature at 2.58 and 2.15 ppm, there may be an equilibrium between the two different dithiolate ring conformations **2a** and **2b** (Scheme 3).

To confirm this, ^1H NMR experiments were recorded at different temperatures. Olefinic protons appear at +30 °C in two broad signals, indicating a fast equilibrium between species **2a** and **2b**. When the temperature is decreased to −60 °C, a slight broadening of these signals can be observed. At −90 °C each signal split into two resonances in an 80:20 ratio with each signal corresponding to one of the conformers. The same behavior was detected in the $^{31}P\{^1H\}$ spectrum at −90 °C.

The X-ray study of complex **2**, discussed below, shows that the least sterically hindered conformer **2a** is the more stable in the solid state. According to these data, we propose that structure **2a** is the main species present in solution at −90 °C.

In an attempt to elucidate the mechanism of the substitution reaction between $[Pt(EDT)(PPh_3)_2]$ and $[Rh(COD)_2]ClO_4$, the ^1H NMR of this mixture was performed at low temperature (−90 °C), but no intermediates could be detected and only the signals corresponding to the starting materials and products were observed.

Crystal Structures of Complexes 1−3, 6, 9, and 12. The crystal structures of complexes **1**−**3**, **6**, **9**, and **12** were determined by X-ray diffraction analysis.

All complexes described here have similar structures, and, as an example, Figure 2 shows the structure for complex **1**. They consist of discrete hetero-binuclear cationic units [(P−P)M(μ-dithiolate)Rh(COD)]$^+$ with the corresponding counteranions ClO_4^-. Cation complexes have a hinged structure where dithiolates act as bridging ligands which coordinate both metals, and the metal centers have square planar rearrangements. The other coordination sites of platinum and palladium centers are occupied by the phosphine ligands, while the rhodium ones are occupied by coordinated COD. Crystal data and selected bond distances and angles are summarized in Tables 1 and 3.

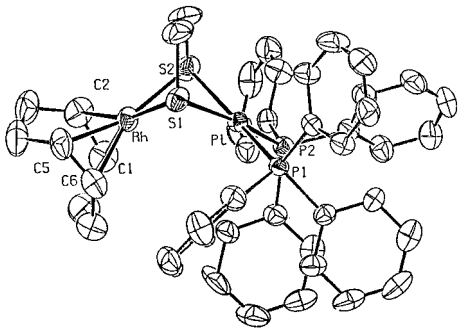

Figure 2. X-ray structure for complex **1** showing thermal ellipsoids at 50% probability.

The rhodium−platinum and rhodium−palladium distances range from 3.0096(6) Å for complex **1** to 3.4084 Å observed for complex **3**. These values are longer than the ones reported for the metal−metal single bond (2.6 Å).[19]

Nevertheless, the Rh···Pt separation for complex **1** (3.0096(6) Å) is one of the shortest reported in the literature and is smaller than that observed for face-to-face Pt···Rh diphenylphosphinoarsino dimers[5a] such as *trans*-[Rh(CO)Cl(μ-dapm)$_2$(*cis*-$PtCl_2$)] (dapm = bis(diphenylarsino)methane) reported by Balch and co-workers, where the Pt···Rh distance was 3.043 Å. In these cases, metal−metal interaction through the out-of-plane orbitals was claimed. For bent structures, the orientation of the out-of-plane orbitals will be less favorable but should not be rejected.

The influence of the size of the dithiolato metalloring in the intermetallic distance can be detected in the complexes containing PPh_3, **1**−**3**. The Pt···Rh distance increases from **1** to **3** according to the number of methylenic carbons between the thiolato groups. This could be attributed to the consistent increasing of the flexibility of the structure.

Intermetallic distances are also sensitive to the phosphine present in the platinum core. The Pt···Rh distances for complexes with the same dithiolato (BDT^{2-}), **3**, **6**, and **9**, increase in the following order: dppp < dppb < PPh_3. This behavior could be attributed to the repulsion between the phenyl groups and the ring constraints.

In the same way, of the BDT^{2-} complexes **3**, **6**, and **9**, those containing PPh_3 (complex **3**) and the seven-membered dppb ring (complex **6**) show the largest P1−Pt−P2 angle (100.8(3) and 100.74(9)°, respectively), while the six-membered dppp ring (complex **9**) has a lower value (96.45(6)°). In contrast, the values of the S−Pt−S, S−Pd−S, and S−Rh−S angles were smaller than 90°, the smallest being the S−Pt−S angle, 78.73(7)°, for complex **1**.

The torsion angle PtS_2Rh θ (Scheme 4, Table 3) changes with the variation in the metal−metal separations. It is smallest for the complex with EDT, **1** (111.27°), and increases as the dithiolato ring increases up to a value of 151.34° for complex **3**. The corresponding homo-dinuclear rhodium(I) dithiolato complexes [Rh(μ-EDT)(COD)]$_2$ and [Rh(μ-PDT)(COD)]$_2$, which we have reported in a previous paper,[10] both had torsion angles of 104°.

The θ values observed for the complexes described in this paper are, in general, slightly larger than the ones reported for homo-binuclear thiolato complexes containing phosphorus-donor ligands. Thus, θ for the phenylthiolato-bridged complex *cis*-

(19) See for example: (a) Farr, J. P.; Olmstead, M. M.; Balch, A. L. *J. Am. Chem. Soc.* **1980**, *102*, 6654. (b) Guimerans, R. R.; Wood, F. E.; Balch, A. L. *Inorg. Chem.* **1984**, 23, 1307.

Table 3. Selected Bond Distances (Å) and Angles (deg) for Complexes **1**−**3**, **6**, **9**, and **12**

	1	**2**	**3**	**6**	**9**	**12**[a]
Pt−P1	2.285(2)	2.297(2)	2.274(7)	2.261(3)	2.243(2)	2.288(2)
Pt−P2	2.267(2)	2.249(2)	2.288(1)	2.260(2)	2.256(2)	2.282(2)
Pt−S1	2.358(2)	2.345(2)	2.341(1)	2.367(2)	2.366(2)	2.368(2)
Pt−S2	2.343(2)	2.332(2)	2.351(1)	2.354(3)	2.259(2)	2.357(2)
Pt−Rh1	3.0096(6)	3.0648(6)	3.4084	3.1984(8)	3.1592(6)	3.1718(7)
Rh−S1	2.372(2)	2.370(2)	2.337(8)	2.352(3)	2.357(2)	2.354(2)
Rh−S2	2.347(2)	2.331(2)	2.358(11)	2.351(2)	2.353(2)	2.352(2)
Rh−M*(C1−C2)[b]	2.030	2.007	2.019	2.039	2.026	2.039
Rh−M*(C5−C6)[b]	2.035	2.022	2.072	2.030	2.039	2.027
P2−Pt−P1	97.25(6)	97.11(6)	100.8(3)	100.74(9)	96.45(6)	100.45(6)
P2−Pt−S2	94.43(7)	91.37(7)	85.2(3)	86.80(10)	89.37(6)	86.20(7)
P1−Pt−S2	168.03(7)	170.09(6)	173.5(3)	172.34(9)	173.78(6)	173.23(6)
P2−Pt−S1	169.78(6)	173.38(6)	164.0(3)	167.76(9)	170.92(6)	168.11(7)
P1−Pt−S1	90.02(6)	88.01(6)	91.5(3)	86.82(9)	87.63(6)	86.37(6)
S2−Pt−S1	78.73(7)	83.17(7)	82.9(3)	85.52(9)	86.29(6)	86.86(6)
S1−Rh−S2	78.38(7)	82.67(7)	82.9(3)	85.95(9)	86.65(6)	87.30(6)
Pt−S1−Rh	79.03(6)	81.08(6)	93.5(3)	85.33(8)	83.96(5)	84.42(6)
Pt−S2−Rh	79.83(6)	82.18(6)	92.7(3)	85.66(8)	84.21(5)	84.68(5)
θ (PtS_2Rh)	111.27	121.42	151.34	135.67	133.62	136.24
φ	96.02	104.91	137.09	129.91	132.30	132.16

[a] Pd complex. [b] M* = medium point between olefinic carbons of COD.

Scheme 4

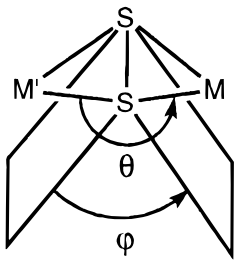

[{Rh(μ-SPh)(CO)(PMe_3)}$_2$] is a value similar to that of complex **2** (113.0°),[9a] but a more sterically demanding thiolate in the iridium complex *cis*-[{Ir(μ-$SCMe_3$)(CO)($P(OMe)_3$)}$_2$] increases this value to 123.2°.[9b]

Another important geometric parameter to be considered is the angle between coordination planes φ without considering the metal coordinates (Scheme 4). In the case of the EDT^{2-} complex (**1**), the value of φ is 96.02°, which is very close to the value for complex [Rh(μ-EDT)(COD)]$_2$ (97°). The difference between the two parameters θ and φ in a particular structure indicates a separation of the metals from their coordination plane. This deviation was also observed for complex [Rh(μ-EDT)(COD)]$_2$ and was attributed to repulsion between metals due to a short metal−metal nonbonding distance.[10]

Metal−ligand distances are in the ranges reported for metal−thiolate−phosphine complexes.[13] Pt−P bond distances in complex **1** (average 2.276 Å) decrease slightly with respect to the corresponding mononuclear dithiolate complex *cis*-[Pt(EDT)-(PPh_3)$_2$] (average 2.2885 Å)[20] but are longer than those for the mononuclear dichlorobis(triphenylphosphine)platinum(II) complex *cis*-[$PtCl_2$(PPh_3)$_2$] (2.251(2) and 2.265(2) Å.).[21] The variation in Pt−P distances is in agreement with the relative values of ^{195}Pt−^{31}P coupling constants (2884.4 Hz for [Pt(EDT)-(PPh_3)$_2$], 3219.9 Hz for complex **1**, and 3513 Hz for [$PtCl_2$(PPh_3)$_2$] measured in $CDCl_3$ with H_3PO_4 as external standard).

The Pt−S and Pd−S bond lengths are not strongly influenced by the variations in Pt−P and Pd−P bond values, which are similar to the ones observed for mononuclear dithiolato−diphosphino complexes.[13c]

As far as the conformation of the metalloring formed in complex **2** is concerned, the crystal structure shows that the methylene β to the thiolato group is oriented toward the rhodium center as in species **2a** (Scheme 3). In agreement with the structure in the solid state, we have proposed that this conformation is the main species observed by NMR in solution.

From the crystallographic data of the complexes discussed here, it can be concluded that simple modifications in the alkyl chain of the bridging dithiolates directly affect geometric parameters such as metal−metal distances and the angles between the coordination planes of the hinged structures. Thus, the platinum−rhodium distance has been modified up to *ca.* 0.4 Å, and there have been variations in the coordination plane angles up to 40°. Similarly, although to a lesser extent, the terminal phosphine position of the platinum or palladium center affects metal−metal distances and angles. These structural changes may influence the chemical properties of these complexes. In addition, further modifications in the electronic properties of the ligands may give these complexes new possibilities of reactivity.

In conclusion, a new route to hetero-bimetallic complexes with bridging dithiolates [(P−P)M(μ-S−S)Rh(COD)]ClO_4 has been set up. The combination of different dithiolates in the bridging position with different ligands in the terminal positions (phosphine and diolefine) may allow the structural and electronic parameters of these complexes to be finely tuned. The catalytic activity in homogeneous processes and the reactivity of these complexes are currently being investigated.

Acknowledgment. We thank the Ministerio de Educación y Ciencia and the Generalitat de Catalunya for financial support (Grant QFN-95-4725-C03-2; CICYT-CIRIT).

Supporting Information Available: Figures showing ORTEP projections of complexes **2**, **3**, **6**, **9**, and **12**, and the ^{1}H NMR spectra of complex **1**, the ^{1}H NMR spectra in the methylenic region of complex **2**, and the ^{31}P{^{1}H} NMR spectrum of complex **2** (8 pages). X-ray crystallographic files, in CIF format, for complexes **1**−**3**, **6**, **9**, and **12** are available on the Internet only. Ordering and access information is given on any current masthead page.

IC970557O

(20) Bryan, S. A.; Roundhill, D. M. *Acta Crystallogr.* **1983**, *C39*, 184.
(21) Ferguson, G.; Anderson, K.; Clark, H. C.; Davies, J. A.; Parvez, M. *J. Crystallogr. Spectrosc. Res.* **1982**, *12*, 449.